

See discussions, stats, and author profiles for this publication at: <https://www.researchgate.net/publication/273785531>

Theoretical study of formamide decomposition pathways over (6,0) silicon-carbide nanotube

ARTICLE *in* JOURNAL OF MOLECULAR MODELING · APRIL 2015

Impact Factor: 1.74 · DOI: 10.1007/s00894-015-2615-3 · Source: PubMed

READS

27

4 AUTHORS, INCLUDING:



Mehdi D Esrafil

University of Maragheh

179 PUBLICATIONS 899 CITATIONS

SEE PROFILE



Parisa Nematollahi

University of Maragheh

7 PUBLICATIONS 0 CITATIONS

SEE PROFILE

Theoretical study of formamide decomposition pathways over (6,0) silicon-carbide nanotube

**Mehdi D. Esrafil, Mozhgan Ghanbari,
Roghaye Nurazar & Parisa Nematollahi**

Journal of Molecular Modeling

Computational Chemistry - Life Science
- Advanced Materials - New Methods

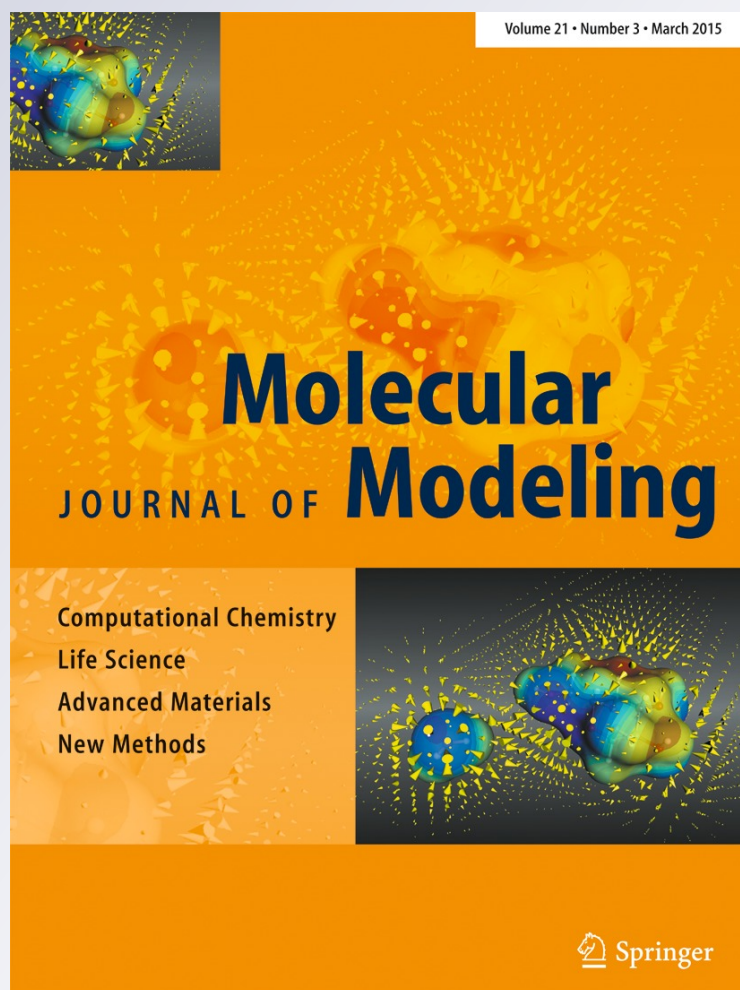
ISSN 1610-2940

Volume 21

Number 4

J Mol Model (2015) 21:1-8

DOI 10.1007/s00894-015-2615-3



Your article is protected by copyright and all rights are held exclusively by Springer-Verlag Berlin Heidelberg. This e-offprint is for personal use only and shall not be self-archived in electronic repositories. If you wish to self-archive your article, please use the accepted manuscript version for posting on your own website. You may further deposit the accepted manuscript version in any repository, provided it is only made publicly available 12 months after official publication or later and provided acknowledgement is given to the original source of publication and a link is inserted to the published article on Springer's website. The link must be accompanied by the following text: "The final publication is available at link.springer.com".

Theoretical study of formamide decomposition pathways over (6,0) silicon-carbide nanotube

Mehdi D. Esrafilī · Mozghan Ghanbari ·
Roghayeh Nurazar · Parisa Nematollahi

Received: 2 November 2014 / Accepted: 8 February 2015
© Springer-Verlag Berlin Heidelberg 2015

Abstract In this study, we systematically identified possible reaction pathways for the catalytic decomposition of formamide (FM) on a (6,0) silicon-carbide nanotube surface by means of density functional theory. To gain insight into the catalytic activity of the surface, the interaction between the FM and SiCNT is analyzed by detailed electronic analysis such as adsorption energy, charge density difference and activation barrier. The energy barriers for the dehydrogenation, decarbonylation, and dehydration processes are found to be in the range of 0.2–49 kcal. Our results indicate that dehydrogenation and decarbonylation pathways are possible routes to get gaseous HNCO, H₂, NH₃, and CO molecules. In contrast, the reaction of HCONH₂→CONH+H presents a large activation energy (about 49 kcal mol⁻¹) which makes the FM dehydration an unfavorable reaction. Moreover, the dehydrogenation appears to be particularly favorable at low temperatures. The theoretical insights gained in this study could be useful for designing and developing metal-free catalysts based on SiC nanostructures.

Keywords Activation energy · Decomposition · DFT · Formamide · SiCNT

Introduction

The adsorption of organonitrogen compounds on different surfaces is very important for their application in catalysis and surface coating chemistry. Formamide (HCONH₂, FM) is the simplest amide which acts as a good model system to

study the surface chemistry of amides [1, 2]. It is also a basic building unit in proteins and the simplest model of nucleic base linkage [3, 4]. FM is the lowest energy isomer of the [CH₃NO] compounds and the simplest stable organic species having the four most common elements. In addition, among small prebiotic precursors, FM has attracted great interest because it can be decomposed to a wide range of smaller stable molecules that are obvious intermediates in prebiotic syntheses such as CO, NH₃, H₂, HNCO, HCHO, H₂O, HCN, and so on. Among these molecules, HCN is the most important segment because its polymerization reactions carried out under a variety of conditions produce different important biomolecules [5, 6].

In recent years, there has been considerable interest in the mechanism of the FM decomposition reaction [7–9]. For example, Kakumoto et al. [10] diluted FM in argon using shock-tube experiments and investigated its thermal decomposition. They found that the decomposition proceeded by the decarbonylation channel. On another hand, mineral surfaces because of their multiple functional groups can connect bimolecular complexes from FM dimers with high energy barrier. Nguyen et al. [11] investigated the possible formation of HCN/HNC from FM. Theoretical studies on the adsorption of FM on both pristine and defective surfaces of pyrite, as a mineral surface, were performed. In addition, the interactions between FM and transition metal surfaces have also been widely studied [12–14]. For the adsorption and decomposition of FM over Ru (0 0 0 1) surface [15], experimental results demonstrated that FM bonds to the surface via the lone pair of electrons on the oxygen atom with Ru centers present at the surface, leaving a mixture of CO, NH₃, NH, and hydrogen adatoms on it. Besides, the results suggested that the exact decomposition route is temperature-dependent. This was found in another work in which Weinberg and coworkers demonstrated that on the Ru (0 0 0 1) surface with a 2×1 oxygen overlayer [16], a different and singular reaction path

M. D. Esrafilī (✉) · M. Ghanbari · R. Nurazar · P. Nematollahi
Laboratory of Theoretical Chemistry, Department of Chemistry,
University of Maragheh, Maragheh, Iran
e-mail: esrafilī@maragheh.ac.ir

is occurred. It reveals that at different temperatures FM adsorbs molecularly from different molecular modes, which finally at high temperatures leads to dissociative adsorption whereby an amino hydrogen dissociates to the surface metal atoms. Nevertheless, high costs and toxicity of transition metal-based catalysts might greatly hinder their applications for FM decomposition. In recent years, there has been an increasing amount of literature on designing new catalysts or additives to solve these problems.

In the present study, a new approach to catalyze the decomposition reaction of the FM molecule using silicon-carbide nanotubes (SiCNTs) is introduced. These nanotubes exhibit many promising properties, such as superior electrical conductivity, excellent mechanical and thermal stability, and so on [17, 18]. Moreover, the advantage of large surface to volume ratio of SiCNTs make them act as a support for heterogeneous catalysts. Through these applications, we interested in metal-free catalysts. For example, recent studies found that SiCNTs could act as an efficient metal-free dehydrogenation catalyst for NH_3BH_3 [19] and hydrazine [20]. Theoretical calculations show that H_2 [21], CO [22], HCN [22], NO [23], and N_2O [23] can be chemically adsorbed on the surface of SiCNTs with larger adsorption energies while it can only physisorbed on the surface of CNTs. Therefore, SiCNTs can be potentially applied as chemical gas sensors. In this work, we employ density functional theory (DFT) calculations to investigate FM adsorption on a finite-size SiCNT. The kinetic parameters of various channels can subsequently be evaluated using calculated geometric, vibrational, and energetic results. The key points that determine the activities of the SiCNT surface for FM decomposition into H_2 , HNCO, NH_3 , CO, HCN, and H_2O species are explained. To our knowledge, no prior theoretical investigations have yet been reported on this issue.

Computational details

We carried out all-electron DFT calculations using standard 6-31G* basis set, implemented in the GAMESS package [24]. Recent studies revealed that the M06-2X density functional is a reliable method for unraveling the non-covalent interactions [25, 26]. Therefore, the same method was used for the present investigation. A truncated (6,0) SiCNT with 42 Si and 42 C atoms was chosen as the basic model for the calculations. In order to avoid the boundary effects, atoms at the open ends of the tube are saturated by hydrogen atoms. Corresponding vibrational frequencies were computed in the harmonic approximation to identify equilibrium and transition structures. All transition state structures were characterized by exhibiting the existence of a single frequency mode associated with a pure imaginary frequency. Intrinsic reaction coordinate (IRC) calculations were performed in the forward and reverse

directions to determine minimum-energy pathways. The adsorption energy (E_{ads}) of adsorbate is calculated using M06-2X/6-31G* method, based on the equation of $E_{\text{ads}}(\text{A}) = E_{\text{A/M}} - E_{\text{M}} - E_{\text{A}}$, where $E_{\text{A/M}}$, E_{M} and E_{A} are the total energies of the adsorbate-substrate system, the substrate, and the energy of the adsorbate in the gas phase, respectively. The natural population analysis [27] was performed at the M06-2X/6-31G* level.

Results and discussion

FM adsorption on the SiCNT

The stable adsorption geometries of a single FM molecule on the SiCNT are first investigated. The optimized geometries of possible adsorption configurations of FM on the SiCNT as obtained from M06-2X/6-31G* level of calculation are shown in Fig. 1, along with geometrical parameters. Also, the same figure contains the electron density difference maps of FM/SiCNT complexes. The calculated adsorption energies, thermodynamic parameters and net charge transfers are listed in Table 1. Various possible adsorption geometries are studied, including when O, N, C, and H atoms of FM molecule are close to either the silicon atom or the carbon atom of the SiCNT. After careful structural relaxation, three stable adsorption configurations were found (A, B, and C). The evaluated E_{ads} values for the formation of FM/SiCNT complexes are all exothermic. In the A configuration, which is the most stable mode, FM molecule is located on the tube surface so that its oxygen atom is close to the Si atom of the SiCNT. The corresponding adsorption energy is about $-46.3 \text{ kcal mol}^{-1}$, which indicates a significant interaction between the FM and the tube surface. The Si–O bonding distance is about 1.80 \AA , that is slightly shorter than the corresponding interaction on Ag (111) [12] and oxygen-covered (0001) surface of ruthenium [14]. The C–N bond length of FM is about 1.30 \AA , a little shorter than that of the isolated molecule (1.36 \AA), suggesting that adsorption process strengthens the C–N bond. Moreover, the N–H distance is elongated from 1.01 \AA in free FM molecule to 1.11 \AA in the complex A. The adsorption process to form complex A is an exothermic reaction ($\Delta H_{298} = -46 \text{ kcal mol}^{-1}$), with a negative ΔG_{298} value of about $-32.6 \text{ kcal mol}^{-1}$ (Table 1). Geometry optimization results also reveal the existence of N–H \cdots C type intermolecular contacts for configuration A. The calculated N–H \cdots C distances is 1.71 \AA which is much shorter than the sum of van der Waals radii of carbon and hydrogen atoms (2.9 \AA) [28]. In this configuration, a small net charge of about 0.13 electrons transfers from FM to the tube. These results are supported by the electron density difference maps depicted in Fig. 1, which indicate a pronounced charge redistribution for the configuration A. In particular, it is found that electrons are depleted from the vicinity of the Si atom and

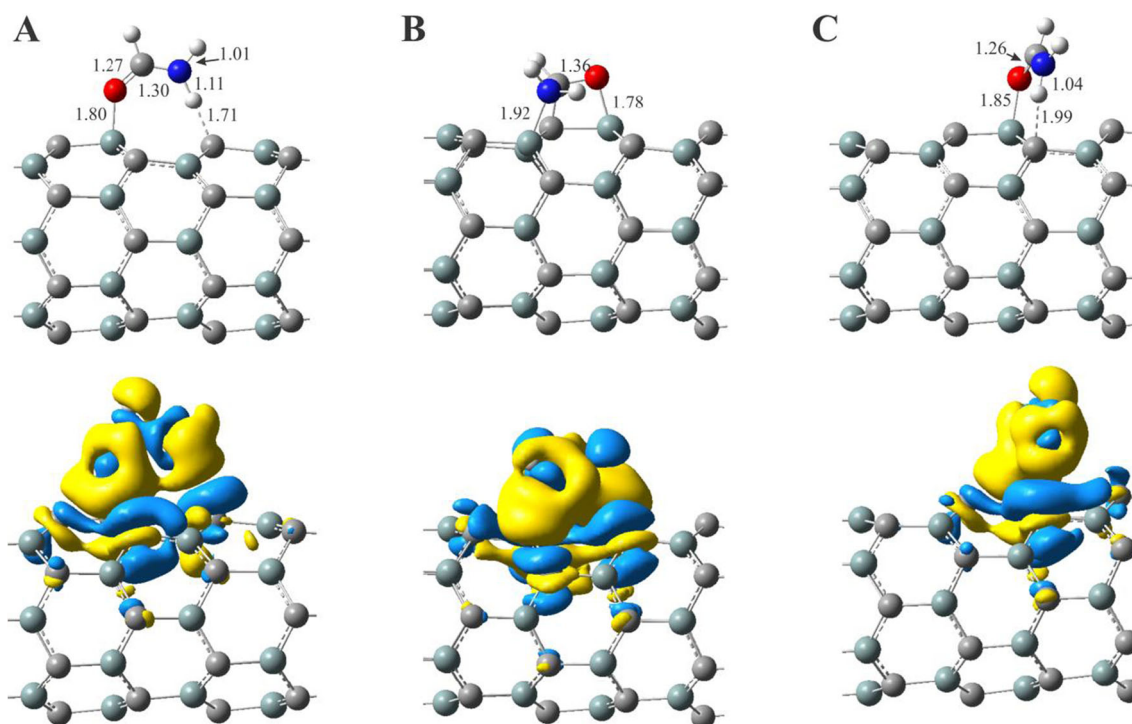


Fig. 1 Optimized structures and corresponding electron density difference maps (0.001 e/bohr^3) of FM/SiCNT complexes. All distances are in Å

are accumulated in the vicinity of the Si–O bond, which confirm the binding between FM and SiCNT induced by adsorption. Besides, the electron density difference map shows that there is a considerable charge transfer and electron density rearrangement associated with the N–H \cdots C hydrogen bond in the configuration A.

Similarly, another chemisorption is found when both C=O and C–N bonds of FM simultaneously attack the Si–C bonds of SiCNT and forms two four-membered rings (i.e., cycloaddition). This mode forms via cleavage of the carbonyl π bond and bonding between the C, O, N atoms of the FM with Si and C atoms of SiCNT. The calculated Si–O bond distance in this configuration (B) is 1.78 Å, which is shorter than that in the A configuration by 0.02 Å. However, the C–N distance is elongated from 1.36 Å in free FM molecule to 1.58 Å in the the complex. The four atoms (H, O, N and surface C) that bond with the C atom of FM compose a tetrahedron, with C as the

center. The elongation of C–N distance and the change of FM configuration indicate that the hybridization of C has varied from sp^2 in free FM to sp^3 in adsorbed FM. Furthermore, the natural charge analysis indicates that the amount of charge transferred from the SiCNT to the π^* anti-bonding orbital of carbonyl group is about 0.20 e which proves the cleavage of carbonyl π bond in FM. According to thermochemistry results, the adsorption process to form complex B is an exothermic reaction ($\Delta H_{298} = -39.6 \text{ kcal mol}^{-1}$), with a negative ΔG_{298} value of about $-24.2 \text{ kcal mol}^{-1}$. As expected, a noticeable charge redistribution is also evident for this adsorption configuration which can be seen in Fig. 1.

In the stable configuration C, the FM molecule is also adsorbed in the top site through its oxygen atom. The calculated adsorption energy is $-34.0 \text{ kcal mol}^{-1}$ and Si–O bond distance is obtained to be 1.85 Å. The N–H bond length of FM is about 1.04 Å, a little longer than that of the isolated molecule (1.01 Å), suggesting that adsorption process activates the N–H bond. An important role in stabilization of this structure is played by the N–H \cdots C nonclassical hydrogen bond between the FM and surface. The process is exothermic with ΔH_{298} and ΔG_{298} values of -32.6 and $-19.7 \text{ kcal mol}^{-1}$, respectively, which indicates a significant thermodynamic stability of FM over the SiCNT surface. The electron density difference maps show that there are considerable charge transfer and electron density rearrangement that mainly associated with Si–O and N–H \cdots C interactions in the C configuration. The deformation of the system structure and the appreciable adsorption energy suggest that the interaction in this configuration belongs to

Table 1 The adsorption energy (E_{ad}), change of Gibbs free energy (ΔG_{298}), change of enthalpy (ΔH_{298}), and net charge transfer (q_{CT}) of FM/SiCNT complexes^a

System	E_{ad} (kcal mol^{-1})	ΔG_{298} (kcal mol^{-1})	ΔH_{298} (kcal mol^{-1})	q_{CT} (e)
A	−46.3	−32.6	−46.0	0.13
B	−41.4	−24.2	−39.6	−0.40
C	−34.0	−19.7	−32.6	0.18

^a q_{CT} from FM to SiCNT

chemisorptions. The adsorption energies obtained from this study are compared with other theoretical studies [12–14] and the FM adsorption configuration matched with those found experimentally over metal surfaces [15]. On the basis of the above discussion, it can be concluded that FM experiences a chemisorption interaction with the SiCNT surface, with a significant change in its structure with respect to the gas-phase molecule.

FM decomposition pathways on the SiCNT

Next, the possibility of FM dissociation on the SiCNT surface is considered. Recently, Nguyen et al. [8] reported on the dehydrogenation, decarbonylation, and dehydration processes of FM in the gas phase. All these channels are competitive with one another and are characterized by comparable energy barriers in the range of 73–78 kcal mol⁻¹. Similarly, the FM molecule can be decomposed on SiCNT surface through the dehydrogenation, decarbonylation, and dehydration pathways. Within this scheme, three different pathways for the FM decomposition have been characterized in detail (denoted as R1, R2, and R3 pathways, respectively), and the energy profiles for these reaction pathways are shown in Fig. 2. The atomic configurations at each state along the reaction pathways are also displayed in Figs. 3, 4, and 5. The corresponding kinetic and thermodynamic parameters are summarized in Table 2.

The reaction pathway R1 begins with the stable configuration A, followed by dehydrogenation of FM into HCONH (Fig. 3). This step has an energy barrier of about 0.20 kcal mol⁻¹ and is exothermic by $\Delta H_{298} = -14.6$ kcal mol⁻¹, which makes the reaction occur rapidly at room temperature. It should be noted that the estimated energy barrier for this step is very low and this may be in the range of inaccuracy of the chosen method. However, the calculated small activation Gibbs free energy (ΔG^\ddagger) and enthalpy (ΔH^\ddagger) values verify

that this reaction step is almost barrierless and can occur easily at room temperature. Next, the HCONH moiety in P1 experiences an endothermic rotation around Si–O bond to form the product P2. The calculations indicate that this step is endothermic ($\Delta H_{298} = 5.5$ kcal mol⁻¹), and an energy-barrier height of approximately 2.3 kcal mol⁻¹, relative to P1, must be overcome. In P2, the bond length of Si–O is about 1.69 Å which is shorter than that in complex A (0.11 Å). The reaction can then proceed with the dissociating of HCONH into an isocyanic acid (HNCO) and a H atom (P3). The relatively high energy-barrier for P2 → P3 reaction can be attributed to the stability of the HCONH moiety over the nanotube surface. The formed HNCO molecule has a weak interaction on the SiCNT substrate (about 4 kcal mol⁻¹), thus it can easily detach from the surface at room temperature. It is noticeable that the initial adsorption energy (–46.3 kcal mol⁻¹) can overcome the C–H bond cleavage barrier (32.3 kcal mol⁻¹). Overall, the C–H splitting on the SiCNT can be considered as the rate-determining step.

The decarbonylation pathway (R2) starts with the elongation of the C–N bond in configuration B, and the resulting stationary structures are shown in Fig. 4. The results indicate that the stable structure B can be converted into the NH₂ and HCO species through a transition state (TS4) with an energy barrier of 3.7 kcal mol⁻¹. The estimated activation free energy and enthalpy are 1.3 and 2.6 kcal mol⁻¹, respectively, which suggests that this reaction is likely to take place rapidly at room temperature. The frequency analysis indicates that TS4 has a single imaginary frequency (283i cm⁻¹), corresponding to the C–N bond cleavage of the adsorbed FM molecule. Likewise, crossing B through TS4, product P4 forms. In the P4, the distance from the N atom of FM to the surface Si atom is 1.74 Å that is shorter than its initial value in B (1.92 Å), which indicates that the nitrogen atom in the P4 approaches closer to the tube surface. However, due to the stable structure of NH₂ on the nanotube, the desorption of NH₂ fragment from

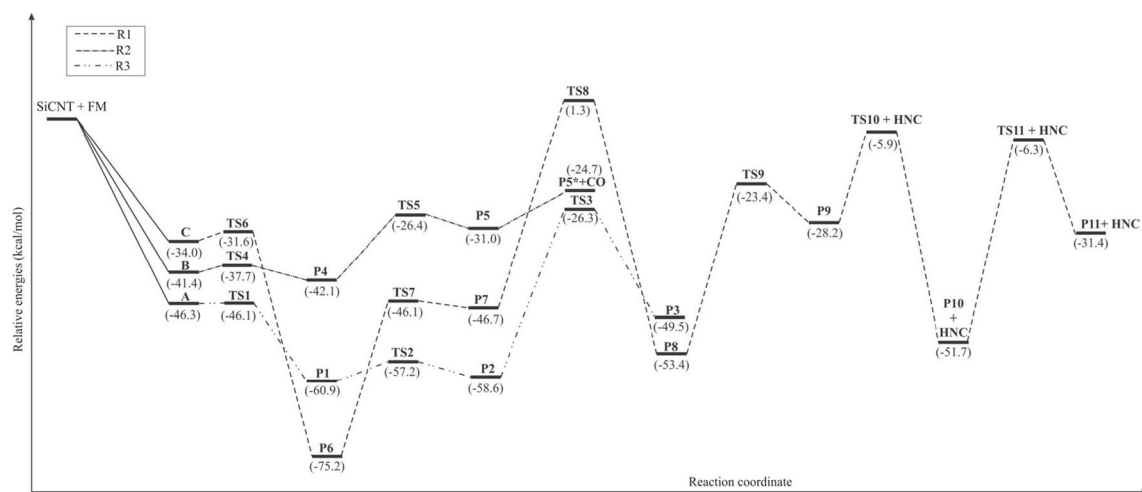


Fig. 2 Reaction pathways of FM decomposition on the (6,0) SiCNT surface

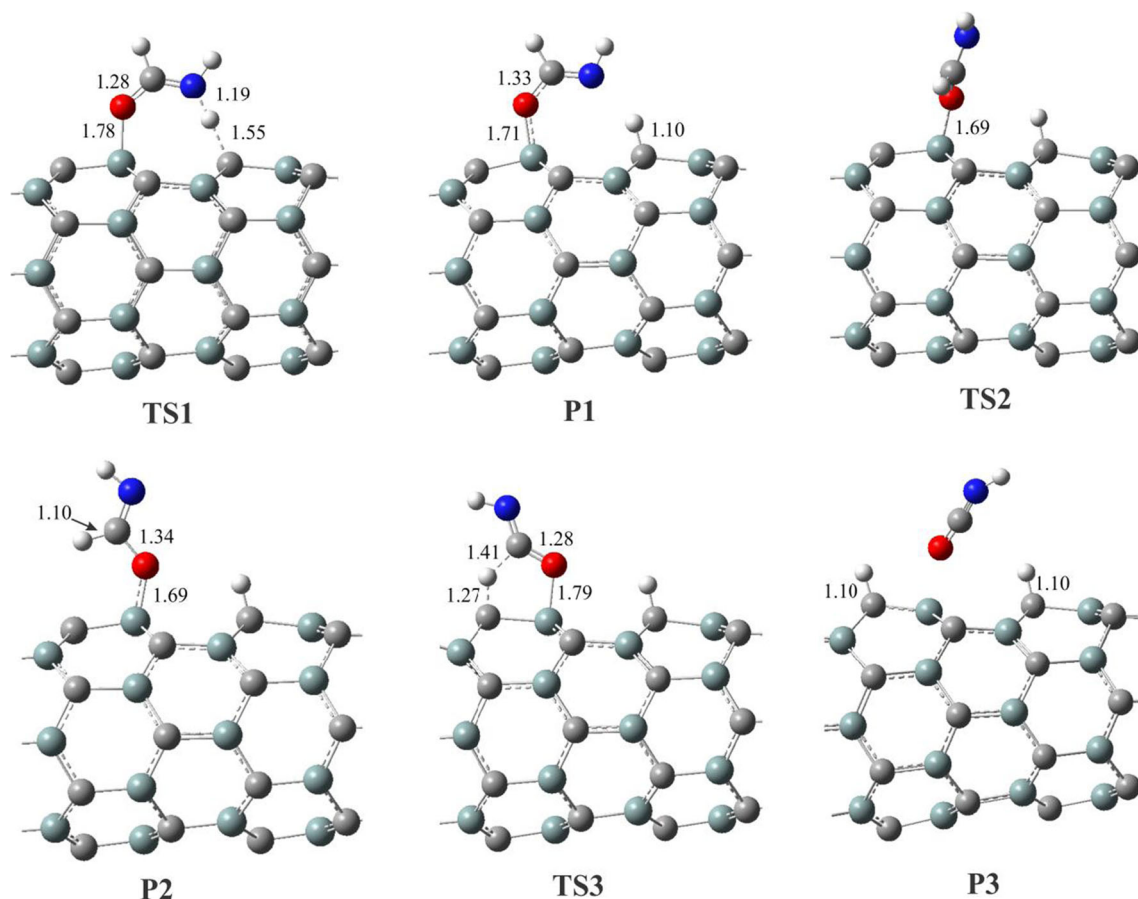


Fig. 3 Optimized structure of stationary points for reaction channels R1. All distances are in Å

the surface is an endothermic reaction with a reaction energy of about 68 kcal mol^{-1} . Then, the reaction can proceed with the dissociating of HC=O into a CO and a H atom (TS5). At the transition state TS5, the C–H bond increased from 1.10 to 1.37 Å , and the distance between the N atom of FM and the Si atom of surface is elongated to 1.83 Å . With the cleavage of C–H bond, the NH_3 and CO molecules are obtained. In P5, the bond lengths of newly formed N–H and Si–N are 1.04 Å and 1.93 Å , respectively. Meanwhile, the obtained intermediate was $-31.0 \text{ kcal mol}^{-1}$ more stable than the $\text{FM} + \text{SiCNT}$ state. The formed CO molecule has a weak interaction on the SiCNT substrate ($6.3 \text{ kcal mol}^{-1}$), thus it can be easily detached from the surface at room temperature. In the final state

(P5*), the length of Si–N is about 1.94 Å and the resulting products ($\text{P5}^* + \text{CO}$) lies at $-24.7 \text{ kcal mol}^{-1}$ with respect to the reactants. It should be noted that the initial adsorption energy ($-31.4 \text{ kcal mol}^{-1}$) cannot overcome the C–H bond cleavage barrier ($32.3 \text{ kcal mol}^{-1}$). Hence, overall, the C–H splitting on SiCNT can be considered as the rate-determining step.

The energy profile of pathway R3 which obtained for dehydration of FM is given in Fig. 2. In this pathway, the configuration C that is presented in Fig. 1 was selected as the initial state. Our DFT calculations indicate that the formation of intermediate P6 is almost spontaneous with a relatively low energy barrier and ΔG^\ddagger values (Table 2). The reaction has a high exothermicity of about $-41.2 \text{ kcal mol}^{-1}$ that makes it

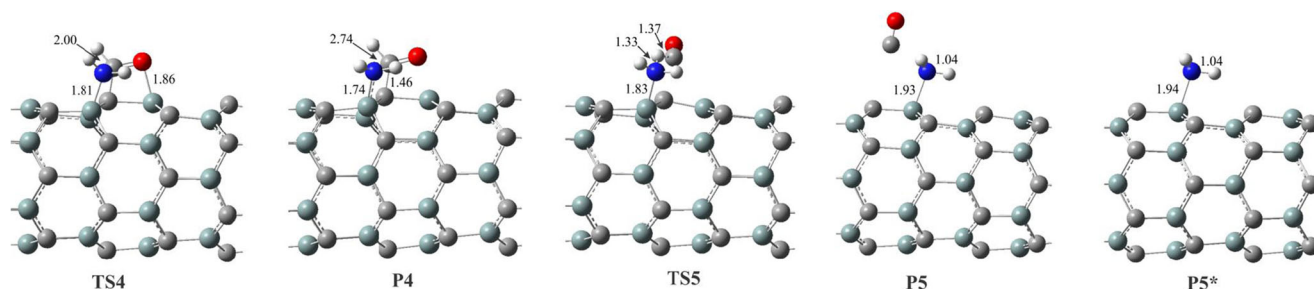


Fig. 4 Optimized structure of stationary points for reaction channels R2. All distances are in Å

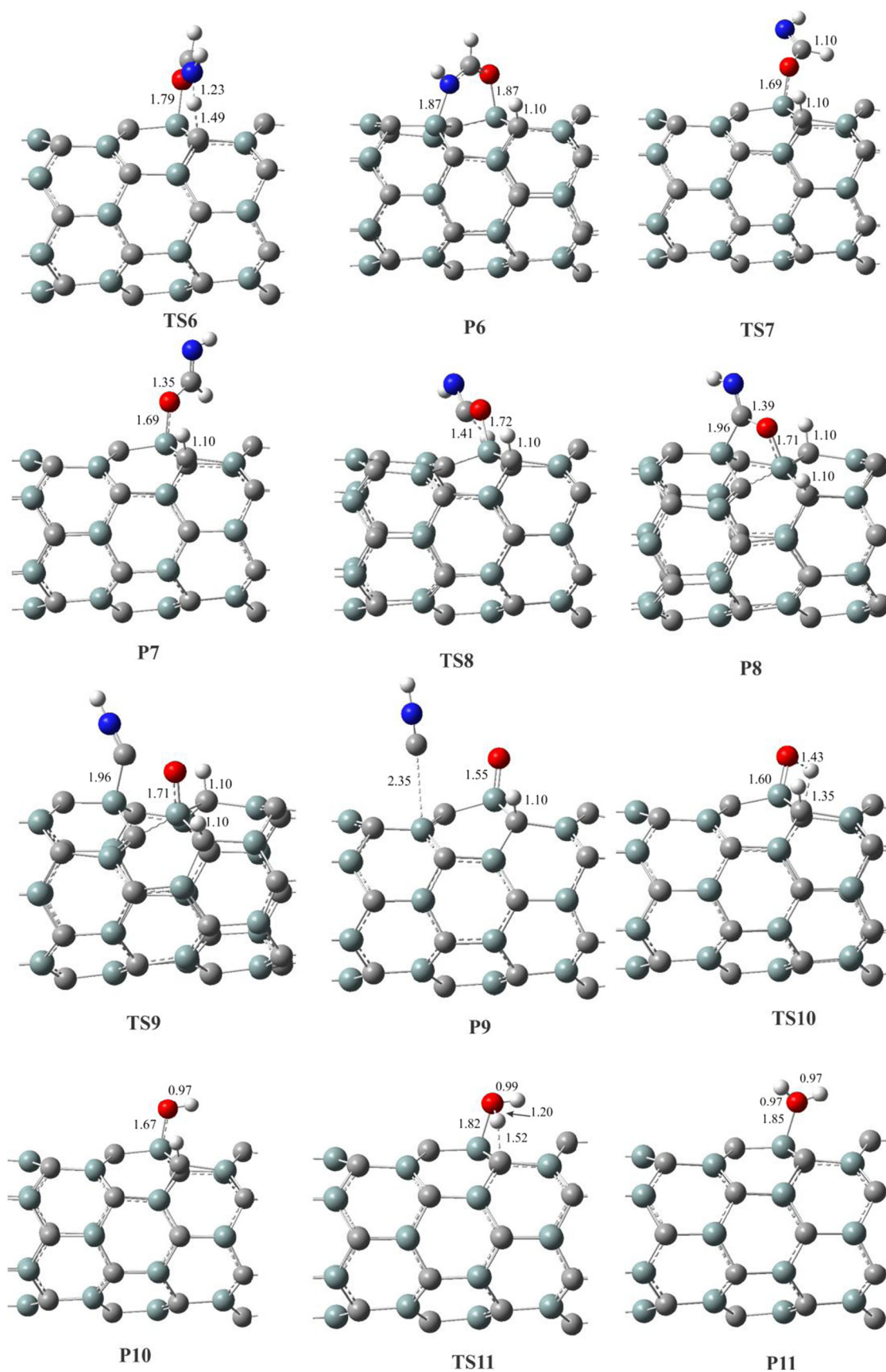


Fig. 5 Optimized structure of stationary points for reaction channels R3. All distances are in Å

Table 2 Calculated activation energy (E_{act}), activation free energy (ΔG^\ddagger), activation enthalpy (ΔH^\ddagger), imaginary frequency (ν), reaction energy (ΔE), change of Gibbs free energy (ΔG_{298}), and change of enthalpy (ΔH_{298}) for different pathways of decomposition of FM on the SiCNT surface^a

Reaction	E_{act}	ΔG^\ddagger	ΔH^\ddagger	ν	ΔE	ΔG_{298}	ΔH_{298}
Pathway R1							
A→P1	0.2	0.1	0.4	647i	-14.6	-14.4	-15.1
P1→P2	2.3	3.3	3.8	16i	5.4	4.9	5.5
P2→P3	32.3	38.1	38.3	961i	3.0	1.6	4.1
Pathway R2							
B→P4	3.7	3.6	3.8	283i	-3.1	-4.0	-2.2
P4→P5	32.2	33.7	34.5	1181i	10.8	8.7	11.8
P5→P5*+CO	-	-	-	-	6.3	-3.6	6.1
Pathway R3							
C→P6	2.4	1.3	2.6	1096i	-40.5	-39.1	-41.2
P6→P7	29.1	27.9	29.5	430i	28.5	26.4	29.3
P7→P8	49.0	50.5	48.3	1513i	-6.8	-5.2	-7.5
P8→P9	30.0	29.4	30.7	117i	54.1	42.6	55.8
P9→P10+HNC	22.3	20.5	19.8	1520i	25.2	-2.5	24.8
P10→P11+HNC	45.4	43.8	43.0	1435i	63.5	53.8	64.7

^a All energies are in kcal mol⁻¹, ν is in cm⁻¹

occur easily. In P6, the HCONH is strongly bound to the Si atom via its O and N atoms ($E_{\text{ads}}=-145$ kcal mol⁻¹), which inhibits its desorption from the SiCNT surface. In the next step, the HCONH moiety in P6 passes through an endothermic rotation around Si–O bond to form the product P7. The calculations indicate that this step is an endothermic and thermodynamically unfavorable reaction ($\Delta G_{298}=26.4$ kcal mol⁻¹), and an energy-barrier height of approximately 29.1 kcal mol⁻¹, relative to P6, must be overcome. The chemically bonded HCONH group may continue to interact with the surface to release another hydrogen atom. The transition state of this step has been located (TS8 in Fig. 5), and the calculated reaction barrier was about 49 kcal mol⁻¹. It has an imaginary frequency of 1513i cm⁻¹, which mainly arises from the dissociated H atom. At the TS8, the C⋯H bond is lengthened to 1.41 Å, and the Si–O distance is only 1.72 Å. In the next step, the hydrogen atom of HCONH group adsorbs on the surface. The obtained intermediate P8 is -53.4 kcal mol⁻¹ more stable than the reactants. Additionally, both adsorptions are accompanied by a relatively strong deformation of the surface. The following step of C–O bond activation needs a reaction barrier of 30.0 kcal mol⁻¹. The structure of the corresponding transition state (TS9) is shown in Fig. 5, where the distance between the C and N atoms is 2.95 Å. Passing over the TS9, the Si–O bond length is continually shortened from 1.71 to 1.55 Å and the Si=O bond gradually tilts, until P9 state is reached, where the formed hydrogen isocyanide (HNC), an O, and two H atoms adsorb on the nanotube surface. Meanwhile, the newly formed

Si–CNH bond length is about 2.35 Å. The formed CNH molecule has thus a weak interaction on the SiCNT surface (5.5 kcal mol⁻¹), and it can be easily detached from the surface at room temperature. Thereafter, the oxygen atom further reacts with the adsorbed hydrogen atoms, as indicated in Fig. 5. Importantly, the results of Table 2 indicate that the reaction of OH+H→H₂O presents a high activation energy (larger than 45.4 kcal mol⁻¹), which makes it an unfavorable reaction. The obtained final state P11 is -31.4 kcal mol⁻¹ more stable than the reactants. Finally, the latter desorbs to produce H₂O in the gas phase and this completes the catalytic cycle.

Conclusions

In this work, the mechanisms of FM decomposition on a SiCNT surface have been systematically investigated by using DFT calculations. The calculated results reveal that SiCNT is able to effectively decompose FM with different mechanisms. Three possible reaction pathways for FM decomposition were proposed. Dehydrogenation and decarbonylation decompositions are possible routes to get gaseous HNCO, H₂, NH₃, and CO molecules. For the dehydration reaction of FM, the HCONH→CONH+H on the SiCNT can be considered as the rate-determining step. The present study is helpful to further widen the potential applications of SiC nanostructures.

Acknowledgments This work was carried out with financial support from the University of Maragheh.

References

- Parmeter JE, Schwalke U, Weinberg WH (1987) J Am Chem Soc 109:1876
- Bu Y, Lin MC (1994) Langmuir 10:3621
- Eschenmoser A, Loewenthal E (1992) Chem Soc Rev 21:1
- Costanzo G, Saladino R, Crestini C, Ciciriello F, Di Mauro E (2007) BMC Evol Biol 7, No. S1.
- Barks HL, Buckley R, Grieves GA, Di Mauro E, Hud NV, Orlando TM (2010) ChemBioChem 11:1240
- Wang J, Gu J, Nguyen MT, Springsteen G, Leszczynski J (2013) J Phys Chem B 117:9333
- Ferus M, Kubelik P, Civis S (2011) J Phys Chem A 115: 12132
- Nguyen VS, Abbott HL, Dawley MM, Orlando TM, Leszczynski J, Nguyen MT (2011) J Phys Chem A 115:841
- Nguyen HT, Nguyen VS, Trung NT, Havenith RWA, Nguyen MT (2013) J Phys Chem A 117:7904
- Kakumoto T, Saito K, Imamura A (1985) J Phys Chem 89: 2286
- Nguyen HT, Nguyen MT (2014) J Phys Chem 118:4079
- Reckien W, Kirchner B, Janetzko F, Bredow T (2009) J Phys Chem C 113:10541
- McGill PR, Sohnel T (2012) J Phys Chem C 116:14368
- Muir JMR, Idriss H (2013) Surf Sci 607:187

15. Parmeter JE, Schwalke U, Weinberg WH (1988) J Am Chem Soc 110:53
16. Parmeter JE, Schwalke U, Weinberg WH (1987) J Am Chem Soc 109:5083
17. Pham-Huu C, Keller N, Ehret G, Ledoux MJ (2001) J Catal 200:400
18. Esrafil MD, Behzadi H (2013) J Mol Model 19:2375
19. Cao F, Sun H (2012) RSC Adv 2:7561
20. Esrafil MD, Mokhtar Teymurian V, Nurazar R (2015) Surf Sci 632:118
21. Mopurmpakis G, Froudakis E, Lithoxoos GP, Samios J (2006) Nano Lett 6:1581
22. Wu RQ, Yang M, Lu HY, Feng YP, Huang ZG, Wu QY (2008) J Phys Chem C 112:15985
23. Gao GH, Kang HS (2008) J Chem Theory Comput 4:1690
24. Schmidt MW, Baldrige KK, Boatz JA, Elbert ST, Gordon MS, Jensen JH, Koseki S, Matsunaga N, Nguyen KA, Su SJ, Windus TL, Dupuis M, Montgomery JA (1993) J Comput Chem 14:1347
25. Esrafil MD, Nurazar R (2014) Superlattice Microst 67:54–60
26. Esrafil MD, Nurazar R (2014) Comput Mater Sci 92:172–177
27. Reed AE, Curtiss LA, Weinhold F (1988) Chem Rev 88:899
28. Bondi A (1964) J Phys Chem 68:441